

Spitzer Observations of Red Galaxies at High Redshifts

Casey Papovich, for the GOODS and MIPS GTO teams

Steward Observatory, 933 N. Cherry Ave., Tucson, AZ 85721

Abstract. I discuss constraints on star-formation and AGN in massive, red galaxies at $z \sim 1-3$ using *Spitzer* observations at $3-24 \mu\text{m}$. In particular I focus on a sample of distant red galaxies (DRGs) with $J-K_s > 2.3$ in the southern Great Observatories Origins Deep Survey (GOODS-S) field. The DRGs have typical stellar masses $M \gtrsim 10^{11} M_\odot$. Interestingly, the majority ($\gtrsim 50\%$) of these objects have $24 \mu\text{m}$ flux densities $\gtrsim 50 \mu\text{Jy}$. At these redshifts massive galaxies undergo intense (and possibly frequent) IR-active phases, which is in contrast to lower-redshift massive galaxies. If the $24 \mu\text{m}$ emission in these $z \sim 1-3$ galaxies is attributed to star formation, then it implies star-formation rates (SFRs) in excess of $\simeq 100 M_\odot \text{ yr}^{-1}$. These galaxies have specific SFRs equal to or exceeding the global average value at that epoch. Thus, this is an active period in their assembly. Based on their X-ray luminosities and near-IR colors, as many as 25% of the massive galaxies at $z \gtrsim 1.5$ host AGN, suggesting that the growth of supermassive black holes coincides with massive-galaxy assembly.

1. Introduction

Most ($\sim 50\%$) of the stellar mass in galaxies today formed during the short time between $z \sim 3$ and 1 (e.g., Dickinson et al. 2003, Rudnick et al. 2003). Much of this stellar mass density resides in massive galaxies, which appear at epochs prior to $z \sim 1-2$ (see, e.g., McCarthy 2004, Renzini 2006). It is still unclear when and where the stars in these galaxies formed. The fashionable scenario is that galaxies “downsize”, with massive galaxies forming most of their stars in their current configuration at early cosmological times, with less-massive galaxies continuing to form stars to the present (e.g., Bauer et al. 2005, Juneau et al. 2005). But it is unclear when and where the stellar mass in galaxies forms. For example, it may be that stars form predominantly in low-mass galaxies at high redshifts, which then merge over time to form large, massive galaxies at more recent times (e.g., Kauffmann & Charlot 1998, Cimatti et al. 2002).

At $z \lesssim 1$ most massive galaxies exist on a fairly prominent red sequence (e.g., Blanton et al. 2003, Bell et al. 2004), are largely devoid of star formation, evolve passively, and contain up to half of the stellar-mass density. However, hierarchical models generally predict colors for massive galaxies at $z \sim 0$ that are too blue compared to observations (e.g., Somerville et al. 2001, Davé et al. 2005). Some recent models suppress star formation in massive galaxies at late times by truncating it at some mass threshold, or by invoking strong feedback from AGN (e.g., Granato et al. 2001, Davé et al. 2005, Croton et al. 2006, Hopkins et al. 2006). The morphologies of the most optically luminous (and the most massive) galaxies transforms from “normal” early-type systems at $z \sim 1$ to irregular systems at $z \sim 2-3$ (e.g., Papovich et al. 2005). To understand the

assembly of these objects we need to study the properties of massive galaxies at these earlier epochs.

In these proceedings, I focus on *Spitzer* observations at 3–24 μm of massive galaxies at $z\sim 1.5\text{--}3$ in the southern Great Observatories Origins Deep (GOODS-S) field. Combined with *HST*/ACS and ground-based data, the *Spitzer* data provide constraints on the star-formation and AGN activity in massive galaxies at these epochs. I discuss the properties of the masses and IR activity in these galaxies, and I comment on the implications for their assembly and evolution.

2. Stellar Masses and Star Formation in High- z Massive Galaxies

GOODS is a multiwavelength survey of two $10'\times 15'$ fields. The GOODS datasets include (along with other things) *HST*/ACS and VLT/ISAAC imaging, *Chandra* X-ray observations (Giavalisco et al. 2004), and recent *Spitzer* imaging (see M. Dickinson’s contribution to these proceedings). I make use of these data for the work described here, as well as data from *Spitzer*/MIPS 24 μm in this field from time allocated to the MIPS GTOs (e.g., Papovich et al. 2004).

Here, I focus on so-called distant red galaxies (DRGs) selected with $J-K_s > 2.3$ mag (Saracco et al. 2001, Franx et al. 2003). This color criterion identifies galaxies at $z\sim 2\text{--}3.5$ whose light is dominated by passively evolving stellar populations older than ~ 250 Myr (i.e., with a strong Balmer/ 4000 Å break between the J and K_s -bands), and also heavily reddened star-forming galaxies at these redshifts (Förster-Schreiber et al. 2004, Papovich et al. 2006). For the GOODS-S data, the $J-K_s > 2.3$ mag selection is approximately complete to stellar masses $\geq 10^{11} M_\odot$ for passively evolving galaxies (see Papovich et al. 2006).

More than 50% of the DRGs have 24 μm detections with $f_\nu(24\mu\text{m}) \geq 50 \mu\text{Jy}$. Daddi et al. (2005), Reddy et al. (2006), and Webb et al. (2006) also find similar 24 μm -detection rates for massive galaxies at $z\sim 2$. Interestingly, this implies that the *majority* of massive galaxies at $z\sim 2$ emit strongly in the thermal IR — *they are either actively forming stars, supermassive blackholes, or both at this epoch*. The 24 μm emission at $z\sim 1.5\text{--}3$ probes the mid-IR ($\sim 5\text{--}10 \mu\text{m}$), which broadly correlates with the total IR, $L_{\text{IR}} \equiv L(8 - 1000\mu\text{m})$ (e.g., Chary & Elbaz 2001). Figure 1 shows the inferred L_{IR} for the DRGs using the Dale et al. (2002) models to convert the observed mid-IR to total IR luminosity. Although there is inherent uncertainty in this conversion, the 24 μm flux densities for the $z\sim 1.5\text{--}3$ DRGs yield $L_{\text{IR}} \approx 10^{11.5\text{--}13} L_\odot$. If attributed to star-formation, then this corresponds to SFRs of $\approx 100\text{--}1000 M_\odot \text{ yr}^{-1}$ (e.g., Kennicutt 1998).

Nearly all of the DRGs are detected in the deep *Spitzer*/IRAC data, implying they have substantial stellar masses. In Papovich et al. (2006), we modeled the DRGs by comparing their ACS, ISAAC, and IRAC $[3.6\mu\text{m}]$ $[4.5\mu\text{m}]$ photometry to stellar-population synthesis models (Bruzual & Charlot 2003). Although the modeling loosely constrains the ages, dust content, and star-formation histories of the DRGs, it provides relatively robust estimates of the galaxies’ stellar masses, which are plotted in figure 1 as a function of redshift. Typical uncertainties for the stellar masses for the full DRG sample are 0.1–0.3 dex.

Figure 2 shows the specific SFRs (Ψ/M) derived from the masses and SFRs for the DRGs, where the SFRs are derived from the summed UV and IR emission. The figure also shows the specific SFRs for lower redshift galaxies from COMBO-17 (Wolf et al. 2003), which overlaps with the GTO 24 μm data.

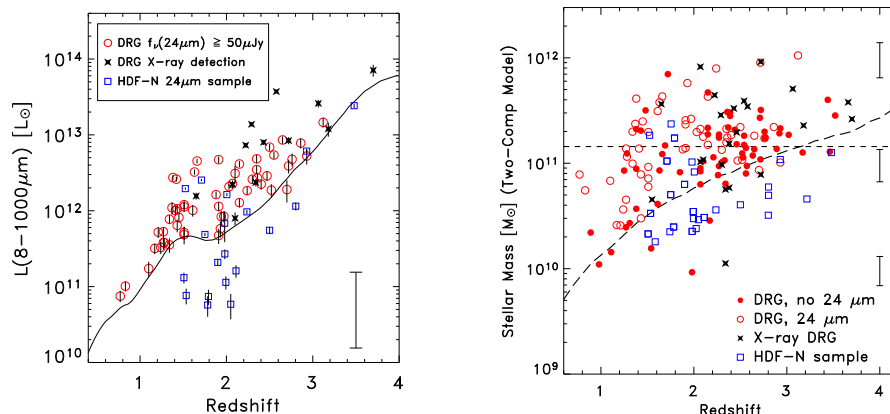


Figure 1. *LEFT*: Total IR luminosities, $L_{\text{IR}} \equiv L(8 - 1000)$, of galaxies inferred from their observed 24 μm emission. Symbol definitions are inset. The solid line denotes the 24 μm 50% completeness limit of the GTO data. The estimated systematic error is ≈ 0.5 dex.. *RIGHT*: Stellar masses of galaxies inferred by fitting models to the galaxies' rest-frame UV-to-near-IR data. The inset bars show the mean errors as a function of mass. The short-dashed line shows the characteristic present-day stellar mass (Cole et al. 2001); the long-dashed line shows the stellar mass limit for a passively evolving stellar population formed at $z \sim \infty$ with $K_s = 23.2$ mag.

The massive galaxies with $M \geq 10^{11} M_\odot$ at $1.5 \leq z \leq 3$ have high specific SFRs, $\Psi/M \sim 0.2-10 \text{ Gyr}^{-1}$ (excluding X-ray sources). In contrast, at $z \lesssim 0.75$ galaxies with $M \geq 10^{11} M_\odot$ have much lower specific SFRs, $\Psi/M \sim 0.1-1 \text{ Gyr}^{-1}$.

In Papovich et al. (2006), we defined the integrated specific SFR as the ratio of the sum of the SFRs, Ψ_i , to the sum of their stellar masses, M_i , $\Upsilon \equiv \sum_i \Psi_i / \sum_i M_i$, summed over all i galaxies. Figure 3 shows the integrated specific SFRs for DRGs at $z \sim 1.5-3.0$ and COMBO-17 at $z \sim 0.4$ and 0.7 , all with $M \geq 10^{11} M_\odot$. The error box indicates the affect of assumptions in the SFRs and AGN activity in the DRGs (see further discussion below, and in Papovich et al. 2006). The integrated specific SFR in galaxies with $M > 10^{11} M_\odot$ declines by more than an order of magnitude from $z \sim 1.5-3$ to $z \lesssim 0.7$.

The curves in figure 2 show the specific SFR integrated over all galaxies (not just the most massive); this is the ratio of the cosmic SFR density to its integral, $\dot{\rho}_* / \int \dot{\rho}_* dt$. Although there is a decrease in the global specific SFR with decreasing redshift, the evolution in the integrated specific SFR in massive galaxies is accelerated. The implication is that *at $z \gtrsim 1.5$, massive galaxies are rapidly forming their stars, whereas by $z \lesssim 1.5$ the specific SFRs of massive galaxies drops rapidly, and lower-mass galaxies dominate the cosmic SFR density*.

3. The Contribution of AGN to the mid-IR Emission

Many ($\sim 15\%$) of the massive galaxies at $z \sim 1.5-3$ are detected in the deep X-ray data, and these objects tend to have high inferred IR luminosities and specific SFRs (see figs. 1 and 2). Indeed, the fraction of X-ray detected DRGs rises with increasing luminosity ($> 50\%$ at $L_{\text{IR}} \gtrsim 10^{13} L_\odot$), similar to the detection

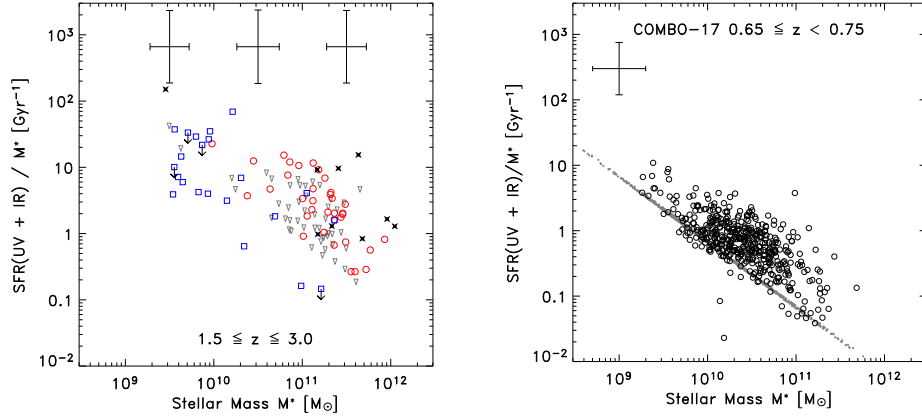


Figure 2. Specific SFRs as a function of galaxy stellar mass. The Left panel shows the DRG and HDF-N galaxies with $1.5 \leq z \leq 3$, with symbols the same as in figure 1. The Right panel shows lower-redshift galaxies from COMBO-17. Open circles show COMBO-17 galaxies with $24 \mu\text{m}$ detections, small filled symbols show upper limits for galaxies undetected at $24 \mu\text{m}$.

rate of sub-mm galaxies (Alexander et al. 2005). At these redshifts the X-ray fluxes imply the presence of an AGN with $L_X \gtrsim 10^{42} \text{ erg s}^{-1}$. Many authors are also finding AGN candidates based on rest-frame near-IR colors, where the AGN is presumably heavily obscured by gas and dust so that it is missed in deep ($\gtrsim 1 \text{ Msec}$) X-ray surveys (e.g., Donley et al. 2005, Stern et al. 2005, Alonso-Herrero et al. 2006, Barmby et al. 2006). Approximately 10% of the X-ray *undetected* DRGs have ACS-through-IRAC colors consistent with dust-enshrouded AGN. Combined with the 15% of DRGs detected in the X-rays, up to 25% of the DRG population host AGN (see also Papovich et al. 2006).

If AGN contribute to the observed $24 \mu\text{m}$ emission in galaxies at $z \sim 1.5-3$, then they can affect the inferred IR luminosities. For example, using an IR template for Mrk 231 instead of a star-forming galaxy with $L_{\text{IR}} \gtrsim 10^{13} L_{\odot}$ would reduce the IR luminosity for $z \sim 1.5-3$ galaxies by a factor of $\sim 2-5$. To limit this effect on the evolution of the integrated specific SFRs, the error box in figure 3 shows how the result changes if for galaxies with putative AGN we set the SFR to zero. The high AGN occurrence in DRGs suggests that massive galaxies at $z \sim 1.5-3$ simultaneously form stars and grow supermassive black holes.

However, even when AGN are present it is unclear whether star-formation or the AGN activity dominates the bolometric IR luminosity. Although $\sim 80\%$ of sub-mm galaxies have X-ray detections (Alexander et al. 2005), the IR to X-ray luminosity ratios are up to an order of magnitude higher than what is expected for AGN alone. This suggests that both star-formation and AGN contribute to the bolometric emission. Similarly, in the near-IR spectrum of a $z \sim 2.5$ DRG, Frayer et al. (2003) find that the galaxy nucleus has a low $\text{H}\alpha$ to $[\text{NII}]$ flux ratio consistent with ionization from an AGN. However, $\text{H}\alpha$ is spatially resolved in their spectrum and the $[\text{NII}]$ line strength drops off in the off-nucleus spectrum. This implies extended star-formation beyond the nucleus, which presumably contributes to the inferred IR luminosity. Both AGN and

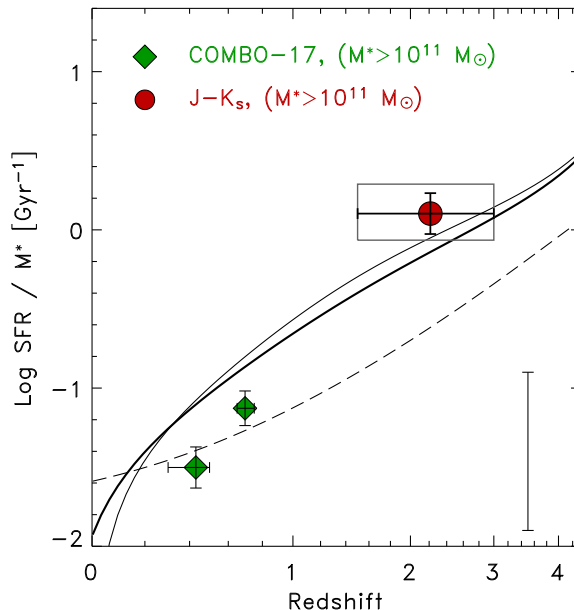


Figure 3. Evolution of the integrated specific SFR, the ratio of the total SFR to the total stellar mass (from Papovich et al. 2006). The curves show the expected evolution from the global SFR density (solid lines, Cole et al. 2001, thick line includes correction for dust extinction; dashed line, Hernquist & Springel 2003). Data points show results for galaxies with $\geq 10^{11} M_{\odot}$. Filled circle corresponds to the DRGs; filled diamonds correspond to the COMBO-17 galaxies. The inset error bar shows an estimate on the systematics.

star-formation occur simultaneously in high-redshift IR-detected galaxies and both probably contribute to the IR emission.

4. Summary

In this contribution, I discussed star-formation and AGN activity in massive galaxies ($\gtrsim 10^{11} M_{\odot}$) at $z \sim 1-3$ using observations from *Spitzer* at $3-24 \mu\text{m}$. The majority ($\gtrsim 50\%$) of these objects have $f_{\nu}(24\mu\text{m}) \geq 50 \mu\text{Jy}$, which if attributed to star formation implies SFRs of $\gtrsim 100 M_{\odot} \text{ yr}^{-1}$. Galaxies at $z \sim 1.5-3$ with $M \geq 10^{11} M_{\odot}$ have specific SFRs equal to or exceeding the global average value. In contrast, massive galaxies at $z \sim 0.3-0.75$ have specific SFRs less than the global average, and more than $10\times$ lower than that at $z \sim 1.5-3$. By $z \lesssim 1.5$ massive galaxies have formed most of their stellar mass, and lower-mass galaxies dominate the SFR density. At the same time, as many as 25% of the massive galaxies at $z \gtrsim 1.5$ host AGN. The high AGN occurrence at $z \sim 1.5-3$ provides evidence that massive galaxies are simultaneously forming stars and growing supermassive black holes. This may provide the impetus for the present-day black-hole-bulge-mass relation and/or provide the feedback necessary to squelch star-formation in such galaxies, moving them onto the red sequence.

Lastly, while on average high-redshift galaxies have IR spectral energy distributions consistent with local templates, individually there remains significant uncertainty. Future work is needed to understand the distribution between the mid-IR (rest-frame 5–15 μm) emission and total IR luminosity in $z \sim 1.5$ –3 galaxies. *Herschel* Space Observatory (and eventually *SAFIR*) will mitigate this problem by measuring the far-IR emission of distant galaxies directly.

Acknowledgments. I wish to thank the conference organizers for the invitation to present this material, and for their work in planning a very successful meeting. I am grateful for my colleagues on the MIPS GTO and GOODS teams for their continued collaboration, in particular I am indebted to L. Moustakas, M. Dickinson, E. Le Floc'h, E. Daddi, and G. Rieke. Support for this work was provided by NASA through the Spitzer Space Telescope Fellowship Program, through a contract issued by JPL/Caltech under a contract with NASA.

References

- Alexander, D. M., Bauer, F. E., Chapman, S. C., et al. 2005, *ApJ*, 632, 736
 Alonso-Herrero, A., et al. 2006, *ApJ*, 640, 167
 Barmby, P., et al. 2006, *ApJ*, in press (astro-ph/0512618)
 Bauer, A. E. et al. 2005, *ApJ*, 621, L89
 Bell, E. F., Wolf, C., Meisenheimer, K., et al. 2004, *ApJ*, 608, 752
 Blanton, M. R., Hogg, D. W., Bahcall, N. A., et al. 2003, *ApJ*, 594, 186
 Bruzual, G. A., & Charlot, S. 2003, *MNRAS*, 344, 1000
 Chary, R. R., & Elbaz, D. 2001, *ApJ*, 556, 562
 Cimatti, A., Daddi, E., Mignoli, M., et al. 2002, *A&A*, 381, L68
 Cole, S., Norberg, P., Baugh, C. M., et al. 2001, *MNRAS*, 326, 255
 Croton, D., Springel, V., White, S. D. M., et al. 2006, *MNRAS*, 365, 11
 Daddi, E. et al. 2005b, *ApJ*, 631, L13
 Dale, D. A., & Helou, G. 2002, *ApJ*, 576, 159
 Davé, R. et al. 2005, preprint (astro-ph/0510625)
 Dickinson, M., Papovich, C., Ferguson, H. C., & Budavári, T. 2003, *ApJ*, 587, 25
 Donley, J. L. et al. 2005, *ApJ*, 634, 169
 Förster-Schreiber, N. M. et al. 2004, *ApJ*, 616, 40
 Franx, M. et al. 2003, *ApJ*, 587, 79
 Frayer, D. et al. 2003, *ApJ*, 126, 73
 Giavalisco, M. et al. 2004, *ApJ*, 600, L93
 Granato, G. L. et al. 2001, *MNRAS*, 324, 757
 Hopkins, P., et al. 2006, preprint (astro-ph/0602290)
 Juneau, S., Glazebrook, K., Crampton, D., et al. 2005, *ApJ*, 619, L135
 Kauffmann, G., & Charlot, S. 1998, *MNRAS*, 294, 705
 Kennicutt, R. C., Jr. 1998, *ARA&A*, 36, 189
 McCarthy, P. 2004, *ARA&A*, 42, 477
 Papovich, C., Dole, H., Egami E., et al. 2004, *ApJS*, 154, 70
 Papovich, C., et al. 2005, *ApJ*, 631, 101
 Papovich, C., Moustakas, L. A., Dickinson, M., et al. 2006, *ApJ*, 640, 92
 Reddy, N. et al. 2006, *ApJ*, in press (astro-ph/0602596)
 Renzini, A. 2006, *ARA&A*, in press (astro-ph/0603479)
 Rudnick, G., Rix, H.-W., Franx, M., et al. 2003, *ApJ*, 599, 847
 Saracco, P., et al. 2001, *A&A*, 375, 1
 Somerville, R. S., Primack, J., & Faber, S. M. 2001, *MNRAS*,
 Stern, D., Eisenhardt, P., Gorjian, V., et al. 2005, *ApJ*, 631, 163
 Webb, T. M. A. et al. 2006, *ApJ*, 616, L17
 Wolf, C. et al. 2003, *A&A*, 401, 73